Intra-bone marrow co-transplantation of umbilical cord mesenchymal stem cells promotes the engraftment of umbilical cord blood stem cells in iron overload NOD/SCID mice

Zhi Huang
Southern Medical University Nanfang Hospital
Yuhua Xiao
Southern Medical University Nanfang Hospital
Xiaomin Chen
Southern Medical University Nanfang Hospital
Huiping Li
Southern Medical University Nanfang Hospital
Jingyu Gao
Southern Medical University Nanfang Hospital
Xinyao Zhang
Southern Medical University Nanfang Hospital
Xiaoqin Feng (fxq126126@126.com)
Southern Medical University Nanfang Hospital

Research

Keywords: Human umbilical cord stem cell, Human umbilical cord mesenchymal stem cells, Intro-Bone marrow injection, Hematopoietic microenvironment

Posted Date: May 8th, 2020

DOI: https://doi.org/10.21203/rs.3.rs-26543/v1

Abstract

Background: Iron overload aggravates the difficulty of umbilical cord blood stem cell engraftment and reduces the survival of patients undergoing hematopoietic stem cells (HSC) transplantation. Mesenchymal stem cells (MSC) have been implicated in playing a significant role in HSC engraftment. This study aimed to determine the effect of intra-bone marrow (IBM) co-transplantation of umbilical cord blood mononuclear cells (UCB-MNC) and mesenchymal stem cells (UC-MSC) on the engraftment and hematopoietic recovery in an iron overload hematopoietic microenvironment.

Methods: The iron overload model was established by dose-escalation intraperitoneal injection of iron dextran in NOD/SCID mice. Iron deposition in the bone marrow, heart, and liver was examined using H&E staining. Serum levels of ferritin and iron status in the liver were measured. The iron overload NOD/SCID mice were sublethally irradiated and divided into four groups for transplantation: (1) control group, (2) IBM MSC+ group: IBM injection of combined UCB-MNC/UC-MSC, (3) IBM group: IBM injection of only UCB-MNC, and (4) IV group: intravenous injection of UCB-MNC. Six weeks after transplantation, the human CD45 + cells in the bone marrow were analyzed by flow cytometry. The semi-quantitative analysis of vascular endothelial growth factor (VEGF-a), osteopontin (OPN), and stromal cell-derived factor-1a (SDF-1a) were examined by immunohistochemistry staining (IHC).

Results: The survival rate and the percentages of human CD45 + cells in bone marrow were highest in the IBM MSC+ group with statistical significance. In addition, the levels of VEGF-a, OPN, and SDF-1a in bone marrow were all significantly higher in the IBM MSC+ group than the other groups.

Conclusion: IBM co-transplantation of UC-MSC might improve the engraftment of UCB-MNC in iron overload NOD/SCID mice. The increased expression of VEGF-a, OPN, and SDF-1a in the bone marrow may be involved in improving the hematopoietic microenvironment and promoting the implantation of human umbilical cord blood stem cells in the bone marrow with iron overload.

Background

Hematopoietic stem cell transplantation (HSCT) is currently the only method that can cure severe-thalassemia and myelodysplastic syndrome [1]. Umbilical cord blood-derived hematopoietic stem cells (UCB-HSC) are emerging as alternative sources of HSC for allogenic HSCT due to their weak immunogenicity and low requirement for HLA matching [2]. However, the clinical application of UCB-HSC is limited due to their small cell numbers and lower implantation rate than other sources of HSC [3]. The engraftment time might be significantly delayed, which increases the risk of infection and death of patients[4]. Repeated blood transfusions also cause tissue iron overload which destroys the hematopoietic microenvironment in the bone marrow and further dampens the efficacy of HSCT[5]. How to promote the implantation of UCB-HSC in the iron-overloaded hematopoietic microenvironment is a challenge to be conquered.

Umbilical cord mesenchymal stem cells (UC-MSC) have been shown to not only have multi-directional differentiation functions but also improve the hematopoietic microenvironment in the bone marrow[6, 7]. This hematopoietic microenvironment is critical for stable and successful implantation of HSC[8]. We hypothesized that co-transplantation of UC-MSC might improve the iron overload-damaged hematopoietic niche to benefit the engraftment of HSCT. The low homing rate of traditional intravenous infusion is another reason causing low engraftment of UCB-HSC[9]. Attempts have been made to use intra-bone marrow (IBM) injection to reduce the loss of cord blood stem cells in non-hematopoietic organs and promote implantation[10]. Therefore, we established an iron-overload murine model to test the effects of IBM co-transplantation of UC-MSC on the engraftment of UCB-HSC.

In this study, we demonstrated that combining UC-MSC transplantation for the IBM HSCT greatly increases the expression of vascular endothelial growth factor (VEGF-a), osteopontin (OPN), and stromal cell-derived factor-1a (SDF-1a) in the iron overloaded bone marrow. Notably, the engraftment of UCB-HSC is significantly enhanced. Our results provide an experimental basis for the feasibility of IBM co-transplantation of MSC and HSC to overcome an iron overload compromised bone marrow hematopoietic niche.

Materials And Methods

Animals

NOD/SCID mice (aged 6 weeks, body weight 20–22 g) were obtained from Beijing Cyagen Biosciences. The mice were housed under specific-pathogen-free (SPF) condition in the Southern Hospital Animal Center. All animal care and experimental procedures were conducted according to ethical standards of animal use and were approved by the Institutional Committee of Animal Care and Use of Southern Medical University.

Reagents and instruments

Iron dextran was purchased from Pharmacosmos (Denmark). RPMI-1640 culture medium and fetal bovine serum (FBS) were purchased from Gibco (US). Lymphocyte separation solution (density 1.077 g/ml) was purchased from TBDsciences (China). DiR fluorescent dye was purchased from Invitrogen (US). Serum ferritin ELISA kit (XY-RS-90F) was purchased from Immunology Consultants Laboratory (US) and iron assay kit (MAK025) from Sigma-Aldrich (US). Immunohistochemistry (IHC) kits were purchased from Leica Biosystems (US). Antibodies against CD45-Bv and CD34-PE-Cy7 were purchased from BD (US), SDF-1a (14-7992-83) from Invitrogen, VEGF-A (ab46154) from Abcam (US), and OPN (AF808) from R&D (US). The inverted microscope was from Olympus (Japan), FACS Calibur flow cytometer from BD (US), and IVIS Spectrum small animal live imager from PerkinElmer (US).

Iron overload mouse model

Fifty-eight female NOD/SCID mice were randomly grouped to control (n = 8), low dose (12.5 mg/ml, n = 42), and high dose (50 mg/ml, n = 8) groups. The control mice were intraperitoneally (i.p.) injected with

normal saline (0.2 ml/injection). The mice of low and high dose groups were i.p. injected with iron dextran (0.2 ml/injection) at indicated concentration, once per every 3 days for 4 weeks. Identification of the iron overload model was assessed by histopathological examination (H&E staining) of iron deposits in the bone marrow, heart, and liver, as well as by measurement of serum ferritin and liver iron.

Measurement of serum ferritin and liver iron

After the establishment of the iron overload model for 4 weeks, the mice in each group were anesthetized by i.p. injection of 0.3% chloral hydrate. Blood collected from the inner canthus vein and the serum was then separated by centrifugation at 1000 × g at 4 °C for 20 minutes. Serum levels of ferritin were determined by using ELISA kit according to the manufacturer's instructions. The fresh liver was harvested and 100 mg of the liver per mouse was used for the measurement of ion levels using an iron assay kit according to the manufacturer's instructions.

Preparation of umbilical cord blood mononuclear cells and mesenchymal stem cells

After obtaining the donor's informed consent, 2 cord blood samples were collected at the time of normal full-term delivery. Single-cell suspensions of mononuclear cells (UCB-MNC) were separated from umbilical cord blood using human lymphocyte separation solution by density gradient centrifugation. For in vivo distribution study, UCB-MNCs were resuspended with normal saline at a concentration of 2×10^7 cells/ml and incubated with a final concentration of DiR at 300 mM for 30 min at 37 °C. Cells were washed twice by centrifugation at 300 × g for 10 min and resuspended with normal saline at 1×10^7 cells/ml. UC-MSC were kind gifts from the Cord Blood Bank of Guangdong Province, China.

Transplantation and examination of engraftment

One week after injection of low dose dextran iron (12.5 mg/ml), the NOD/SCID mice were irradiated with ^{60}Co 2.7 Gy. Six hours after the irradiation, the mice were divided into 4 groups: control group (n = 8) receiving only normal saline (200 μl/mouse) via intravenous (tail vein) injection, IBM MSC + group (n = 11) receiving UCB-MNC plus UC-MSC via IBM (intra-tibial) injection, IBM group (n = 10) receiving only UCB-MNC via IBM (intra-tibial) injection, and IV group (n = 10) receiving only UCB-MNC via intravenous (tail vein) injection. To examine the engraftment rate, after 6 weeks of transplantation, peripheral blood and bone marrow were collected. After incubation with RBC lysis buffer, the samples were incubated with anti-CD45-BV510 to analyze the human-derived cells. Human $CD45^+$ cells greater than 0.1% was considered as successful transplantation.

Immunohistochemistry (IHC) staining and semi-quantitative scoring

Six weeks after the transplantation, femur samples were harvested, fixed with 10% formaldehyde, and embedded in paraffin. Serial sections (2-μm-thick) of each sample were processed immunohistochemically for the expression of OPN, VEGF-a, and SDF-1a using IHC kits according to the

manufacturer's instruction. Briefly, tissue sections were deparaffinized, rehydrated, and blocked for endogenous hydrogen peroxide activity. Antigen retrieval was performed in EDTA buffer with a microwave oven. The primary and secondary antibodies were sequentially applied and incubated in a humidity box at 37 °C for 30 min and 40 min, respectively, followed by developing in DAB solution for 1–2 minutes. Sections were counterstained with hematoxylin solution for 4 min. The positive expression of OPN, VEGF-a, and SDF-1a were found in the cytoplasm and cell membrane and shown as brownish staining, which was semi-quantitatively assessed by scoring the proportion and intensity of stained cells according to published methods of T Padro et al. [11]. Briefly, the percentage of positive cells stained with each specific antibody within cellular areas was estimated according to a three-grade scale (1 = < 10% positive cells, 2 = 10–50% positive cells, 3 = > 50% positive cells). The degree of cellular staining intensity was defined in the following manner: 0 = faint or negative, 1 = light, 2 = moderate, 3 = intense. The score of each sample was obtained by observing 10 fields at high power (400×) magnification using an inverted microscope. The mean of cellular staining intensity was multiplied with the number obtained when estimating the percentage of positive cells according to the three grade scales. The results were expressed as arbitrary units (AU).

Statistical analysis

All experiments were performed at least three times. Differences were compared using student's *t*-tests. The statistical analyses were performed with SPSS software (version 10.0).

Results

Establishment and identification of iron-overload murine model

The iron overload murine model was established by intraperitoneal injection of escalating doses of iron dextran to NOD/SCID mice. The mortality rate of the high dose group reached 60% and no mortality was observed in the low dose group. Four weeks after iron dextran injection, dose-dependent iron deposits could be easily observed in the bone marrow, heart, and liver by using H&E staining (Fig. 1A). Dose-dependent tissue destructions were also observed. Compared with the control group, the injection of iron dextran induced the increased lipid vacuoles in the bone marrow, disorientation of cardiac muscle fibers, and distortion of the hepatic sinus. Iron status in the liver (Fig. 1B) and serum level of ferritin (Fig. 1C) were significantly increased by the injection of iron dextran in a dose-dependent manner. Taken together, these results demonstrated that this experimental murine model reflected an iron-overloaded pathogenic condition.

Survival of the recipient mice

Due to the high mortality rate of iron overload mice induced by a high dose of iron dextran, we therefore chose the low dose model to perform cell transplantation. After transplantation, all mice in the control

group died due to bone marrow failure and internal bleeding (median survival time: 11 days). Six weeks after transplantation, the survival rates of control, IV, IBM, and IBM MSC + groups were 0% (0/8), 60% (6/10), 60% (6/10), and 83% (10/11), respectively. The survival rate of the IBM MSC + group was highest but the statistical difference to the IBM group ($P = 0.091$) or IV group ($P = 0.087$) was not reached. There was no statistical difference in the survival rate between IBM and IV group ($P = 0.925$).

Migration and distribution of UCB-MNC in vivo

To investigate the organ distribution of UCB-MNC after transplantation, DiR-labeled UCB-MNCs were injected and traced using in vivo fluorescence imaging. On the day of transplantation (Fig. 2A), both groups showed high fluorescence intensity in the injection sites, including the tail vein of the IV group and tibia of the IBM group. Six weeks after transplantation, the IV group showed the labeled UCB-MNCs were accumulated in the spleen but not in the bone marrow (Fig. 2B), whereas the IBM group showed accumulation of UCB-MNCs was mainly in the bone marrow.

Verification of engraftment efficacy

To confirm the efficacy of UCB-MNC engraftment, six weeks after transplantation, the bone marrow of 22 survived mice was harvested and examined by the content of human $CD45^+$ cells. Flow cytometry results showed the % of human $CD45^+$ cells in the bone marrow of MSC+, IBM, and IV groups was 9.7%±1.86%, 4.1 ± 1.6%, and 4.5 ± 1.26%, respectively (Fig. 3A-C). The human $CD45^+$ cells were significantly higher in the IBM MSC + group when compared to the other two groups (Fig. 3D). No significant difference was found between IBM and IV groups (Fig. 3D). The results indicated co-transplantation of UC-MSC could significantly enhance the engraftment rate of UCB-MNC in the iron overload microenvironment.

Expression of VEGF-a, OPN, and SDF-1a in the bone marrow

Next, the expression of hematopoiesis cytokines in the bone marrow was investigated. After 6 weeks of transplantation, the femur of 22 survived mice was harvested and examined by IHC staining for the expression of VEGF-a, OPN, and SDF-1a (Fig. 4). The bone marrow of the control group showed increased lipid vacuoles and decreased hematopoietic cells. The expression of VEGF-a, OPN, and SDF-1a was very weak in the control group but notably higher in the IBM MSC + group. The semi-quantitative results were shown in Table 1. The results indicated co-transplantation of UC-MSC might promote engraftment of UCB-MNC via upregulation of hematopoiesis cytokines in the hematopoietic microenvironment.

Table 1
Expression of VEGF-a, OPN, and SDF-1a in the bone marrow of each group

		VEGF-a (AU)	OPN (AU)	SDF-1a (AU)
IBM MSC+	n = 10	3.56	3.33	2.22
IBM	n = 6	1.17	1.67	1.17
IV	n = 6	1.33	1.5	1.17
Control	n = 1	1	1	1

Discussion

Hematopoietic stem cell transplantation (HSCT) is increasingly used as a curative therapy for a variety of disorders of the hematopoietic and immune systems. Recipients of HSCT frequently have iron overload resulting from chronic transfusion therapy for anemia, especially in patients with myelodysplastic syndromes and thalassemia. In this study, we established an iron overload NOD/SCID model to create a bone marrow microenvironment in which the hematopoietic niche was impaired. In these iron overload NOD/SCID mice, IBM co-transplantation of UC-MSC and UCB-MNC significantly promotes the engraftment of UC-MNC when compared with the group receiving IBM transplantation of only UC-MNC. To our knowledge, this is the first study reporting the novel approach of IBM co-transplantation of UC-MSC and UCB-MNC and showing the improved engraftment efficacy. Since the UC-MSC is easy to be obtained without invasive procedures and could be used with high compatibility due to its weak antigenicity, this study provided an insight on the feasibility and benefits of UC-MSC co-transplantation in HSCT.

In addition, IBM injection showed remarkable effects on the homing of HSC. Six weeks after the transplantation of DiR-labeled UC-MNC, the in vivo fluorescence imaging was performed. The IBM injection (IBM) group showed the retention of transplanted DiR-labeled UC-MNC in the bone marrow, whereas the intravenous (IV) group showed the transplanted cells were mainly accumulated in the spleen. The results suggested that IBM injection might be able to reduce the loss of HSC in the reticuloendothelial system and promote the homing of HSC. This finding was inconsistent with previous reports showing IBM is an effective approach for HSCT compared to traditional IV transplantation [10, 12, 13]. However, we found there was no difference between IBM and IV groups regarding the engraftment rate of UCB-MNC when using the iron overload model. The reason causing this discrepancy might be that the impairment of the hematopoietic niche by iron overload might affect the engraftment rate of HSCT conducted by different methods. Nevertheless, here we suggested even in an iron overloaded condition, IBM co-transplantation of MSCs might be a feasible approach to overcome the compromised hematopoietic microenvironment to achieve successful HSCT.

The debilitating effect of iron overload has been indicated by the increasing clinical evidence that iron overload has a suppressive effect on hematopoiesis in myelodysplastic syndromes or anemia patients and that iron chelation therapy could improve this situation[14, 15]. Iron overload markedly decreased the ratio and clonogenic function of murine HSC progenitors by the elevation of reactive oxygen species (ROS). Reducing the ROS level improved the long-term and multi-lineage engraftment of HSC after transplantation[16]. Iron accumulation in the bone marrow niche of thalassemia patients which might increase ROS production to impair the most primitive MSC pool as well as MSC stemness. A weakened antioxidative response and diminished expression of bone marrow niche-associated genes in the MSC were found. This caused a functional impairment in MSC hematopoietic supportive capacity in vitro and in vivo[17]. Since the beneficial effects of MSC were hampered by iron overload, we, therefore, replenished the MSC pool by IBM co-transplantation of MSC with HSC. In agreement, this approach is successful in overcoming the iron overload-mediated impairment of hematopoiesis capacity. Whether ROS involves the beneficial effects is worth of further investigation.

MSCs are important in the regulation of hematopoietic stem cell niche due to their self-renewal and differentiation capacity into tissues of mesodermal origin. These MSC derivatives support hematopoiesis through release various molecules that play a crucial role in migration, homing, self-renewal, proliferation, and differentiation of HSC[18]. For example, MSC could differentiate to osteoblasts which are closely related to the successful engraftment of stem cells [19, 20]. MSC also secrete extracellular matrices such as aminoglycan and proteoglycan and maintain the hematopoietic microenvironment by releasing soluble factors for the interaction between cells[21, 22]. Different subtypes of MSC interact with hematopoietic stem cells in specific areas around blood vessels. $CD271^+$ and $CD271^+/CD146^{-/low}$ MSCs are described as bone lining cells associated with long-term hematopoietic stem cells in the hypoxic region of bone marrow. $CD146^+$ and $CD271^+/CD146^+$ MSCs are located in the perivascular regions of the bone marrow sinus and related to the activation and proliferation of hematopoietic progenitor stem cells[23]. Specific subsets of MSC might be considered for the co-transplantation therapy of MSC and HSC to further improve the engraftment efficacy.

Mechanistically, our study found co-transplantation with UC-MSC significantly increased the expression of VEGF-a, OPN, and SDF-1a in the bone marrow, which might be closely related to the paracrine effect of MSC. VEGF-a, a critical factor for angiogenesis, also mediates the proliferation and migration of osteoblasts[24]. Previous studies found that the beneficial effects of VEGF-a on stem cells might be via inhibition of irradiation-induced apoptosis and facilitation of cell survival by paracrine effect[25, 26]. Bone marrow morphogen osteopontin (OPN), which is abundantly present in the bone marrow extracellular matrix, can maintain hematopoietic stem cell reconstitution potential and the progenitor pool in the bone marrow[27, 28]. SDF-1/CXCR4 axis is indispensable to the homing of HSC[29, 30]. The collective effects of increased expression of VEGF-a, OPN, and SDF-1a induced by co-transplantation of UC-MSC might be multifactorial and beneficial for the reconstitution of bone marrow hematopoietic niche. In the bone marrow sections of the IBM MSC + group, the higher cellularity of hematopoietic cells and fewer lipid vacuoles also indicated the role of UC-MSC in tissue regeneration and repair for iron

overloaded bone marrow microenvironment. This study provided a feasible therapeutic strategy as well as an experimental model that could be used for further study on finding a better treatment for the iron overloaded patients with hematopoietic dysfunction.

Abbreviations

HSCT: Hematopoietic stem cell transplantation; UCB-HSC: Umbilical cord blood-derived hematopoietic stem cells; UC-MSC: Umbilical cord mesenchymal stem cells; SDF-1a: stromal cell-derived factor-1a; SPF: specific-pathogen-free; *IHC: Immunohistochemistry;* AU: arbitrary units; HSCT: Hematopoietic stem cell transplantation; IV: intravenous; ROS: reactive oxygen species; OPN: osteopontin

Declarations

Ethics approval and consent to participate

All animal care and experimental procedures were conducted according to ethical standards of animal use and were approved by the Institutional Committee of Animal Care and Use of Southern Medical University. Consent to participate is not applicable.

Consent for publication

Not applicable.

Availability of data and materials

All the data and material have been presented in the main paper.

Competing interests

The authors declare that they have no competing interests.

Funding

This work was supported by the grant from the Guangdong Science and Technology Department of Guangdong province, China [2014A020211021].

Authors' contributions

We declare that all the listed authors have participated actively in the study and all meet the requirements of the authorship. ZH performed analysis, transplantation of the cord blood stem cells in mice and statistics of the data of the research, participated writing the manuscript. XH and XC performed the animal model of iron overload, ICH of bone marrow and finished ELISA test. HL and JG performed the

histological examination of the liver, heart and bone marrow. XZ collected specimens and research data. XF designed the protocol of the research and was a major contributor in writing the manuscript. All authors read and approved the final manuscript.

Acknowledgements

None declared.

References

1. Li C, Wu X, Feng X, He Y, Liu H, Pei F, et al. A novel conditioning regimen improves outcomes in β-thalassemia major patients using unrelated donor peripheral blood stem cell transplantation. Blood. 2012;120:3875–81.
2. Park SK, Won JH. Usefulness of umbilical cord blood cells in era of hematopoiesis research. Int J Stem Cells. 2009;2:90–6.
3. Eapen M, Rocha V, Sanz G, Scaradavou A, Zhang MJ, Arcese W, et al. Effect of graft source on unrelated donor haemopoietic stem-cell transplantation in adults with acute leukaemia: A retrospective analysis. Lancet Oncol. 2010;11:653–60.
4. Montoro J, Piñana JL, Moscardó F, Sanz J. Infectious complications after umbilical cord-blood transplantation from unrelated donors. Mediterr. J. Hematol. Infect. Dis. 2016. p. e2016051.
5. Pullarkat V. Iron overload in patients undergoing hematopoietic stem cell transplantation. Adv. Hematol. 2010. p. pii: 345756.
6. Nishikawa E, Matsumoto T, Isige M, Tsuji T, Mugisima H, Takahashi S. Comparison of capacities to maintain hematopoietic stem cells among different types of stem cells derived from the placenta and umbilical cord. Regen Ther. 2016;4:48–61.
7. Kim A, Shim S, Kim MJ, Myung JK, Park S. Mesenchymal stem cell-mediated Notch2 activation overcomes radiation-induced injury of the hematopoietic system. Sci Rep. 2018;8:9277.
8. Smith JNP, Calvi LM. Concise review: Current concepts in bone marrow microenvironmental regulation of hematopoietic stem and progenitor cells. Stem Cells. 2013. p. 1044–50.
9. Cui J, Wahl RL, Shen T, Fisher SJ, Recker E, Ginsburg D, et al. Bone marrow cell trafficking following intravenous administration. Br J Haematol. 1999;107:895–902.
10. Kushida T, Inaba M, Hisha H, Ichioka N, Esumi T, Ogawa R, et al. Intra-bone marrow injection of allogeneic bone marrow cells: A powerful new strategy for treatment of intractable autoimmune diseases in MRL/lpr mice. Blood. 2001;97:3292–9.
11. Padró T, Bieker R, Ruiz S, Steins M, Retzlaff S, Bürger H, et al. Overexpression of vascular endothelial growth factor (VEGF) and its cellular receptor KDR (VEGFR-2) in the bone marrow of patients with acute myeloid leukemia. Leukemia. 2002;16:1302–10.
12. Chen C, Su Y, Chen J, Zhang D, Song Y, Guo S. Intra-bone marrow transplantation of endosteal bone marrow cells facilitates allogeneic hematopoietic and stromal cells engraftment dependent on early

expression of CXCL-12. Med Sci Monit. 2015;21:2757–66.

13. Lange S, Steder A, Killian D, Knuebel G, Sekora A, Vogel H, et al. Engraftment Efficiency after Intra–Bone Marrow versus Intravenous Transplantation of Bone Marrow Cells in a Canine Nonmyeloablative Dog Leukocyte Antigen-Identical Transplantation Model. Biol Blood Marrow Transplant. 2017;23:247–54.
14. Pullarkat V. Objectives of iron chelation therapy in myelodysplastic syndromes: More than meets the eye? Blood. 2009. p. 5251–5.
15. Lee SE, Yahng SA, Cho BS, Eom KS, Kim YJ, Lee S, et al. Improvement in hematopoiesis after iron chelation therapy with deferasirox in patients with aplastic anemia. Acta Haematol. 2013;129:72–7.
16. Chai X, Li D, Cao X, Zhang Y, Mu J, Lu W, et al. ROS-mediated iron overload injures the hematopoiesis of bone marrow by damaging hematopoietic stem/progenitor cells in mice. Sci Rep. 2015;5:10181.
17. Crippa S, Rossella V, Aprile A, Silvestri L, Rivis S, Scaramuzza S, et al. Bone marrow stromal cells from β-thalassemia patients have impaired hematopoietic supportive capacity. J Clin Invest. 2019;129:1566–80.
18. Aqmasheh S, Shamsasanjan K, Akbarzadehlaleh P, Sarvar DP, Timari H. Effects of mesenchymal stem cell derivatives on hematopoiesis and hematopoietic stem cells. Adv. Pharm. Bull. 2017. p. 165–77.
19. Calvi LM, Adams GB, Weibrecht KW, Weber JM, Olson DP, Knight MC, et al. Osteoblastic cells regulate the haematopoietic stem cell niche. Nature. 2003;425:841–6.
20. Hanna H, Mir LM, Andre FM. In vitro osteoblastic differentiation of mesenchymal stem cells generates cell layers with distinct properties. Stem Cell Res Ther. 2018;9:203.
21. Phinney DG, Prockop DJ. Concise Review: Mesenchymal Stem/Multipotent Stromal Cells: The State of Transdifferentiation and Modes of Tissue Repair-Current Views. Stem Cells. 2007;25:2896–902.
22. Van Poll D, Parekkadan B, Cho CH, Berthiaume F, Nahmias Y, Tilles AW, et al. Mesenchymal stem cell-derived molecules directly modulate hepatocellular death and regeneration in vitro and in vivo. Hepatology. 2008;47:1634–43.
23. Tormin A, Li O, Brune JC, Walsh S, Schütz B, Ehinger M, et al. CD146 expression on primary nonhematopoietic bone marrow stem cells is correlated with in situ localization. Blood. 2011;117:5067–77.
24. Midy V, Plouet J. Vasculotropin/vascular endothelial growth factor induces differentiation in cultured osteoblasts. Biochem Biophys Res Commun. 1994;199:380–6.
25. Gerber HP, Malik AK, Solar GP, Sherman D, Liang XH, Meng G, et al. VEGF regulates haematopoietic stem cell survival by an internal autocrine loop mechanism. Nature. 2002;417:954–8.
26. Katoh O, Kawaishi K, Kimura A, Satow Y, Tauchi H. Expression of the Vascular Endothelial Growth Factor (VEGF) Receptor Gene, KDR, in Hematopoietic Cells and Inhibitory Effect of VEGF on Apoptotic Cell Death Caused by Ionizing Radiation. Cancer Res. 1995;55:5687–92.

27. Li J, Carrillo García C, Riedt T, Brandes M, Szczepanski S, Brossart P, et al. Murine hematopoietic stem cell reconstitution potential is maintained by osteopontin during aging. Sci Rep. 2018;8:2833.
28. Cao H, Cao B, Heazlewood CK, Domingues M, Sun X, Debele E, et al. Osteopontin is An Important Regulative Component of the Fetal Bone Marrow Hematopoietic Stem Cell Niche. Cells. 2019;8:985.
29. Peled A, Petit I, Kollet O, Magid M, Ponomaryov T, Byk T, et al. Dependence of human stem cell engraftment and repopulation of NOD/SCID mice on CXCR4. Science (80-). 1999;283:845–8.
30. Lapidot T, Kollet O. The essential roles of the chemokine SDF-1 and its receptor CXCR4 in human stem cell homing and repopulation of transplanted immune-deficient NOD/SCID and NOD/SCID/B2mnull mice. Leukemia. 2002;p. 16:1992–2003.

Figures

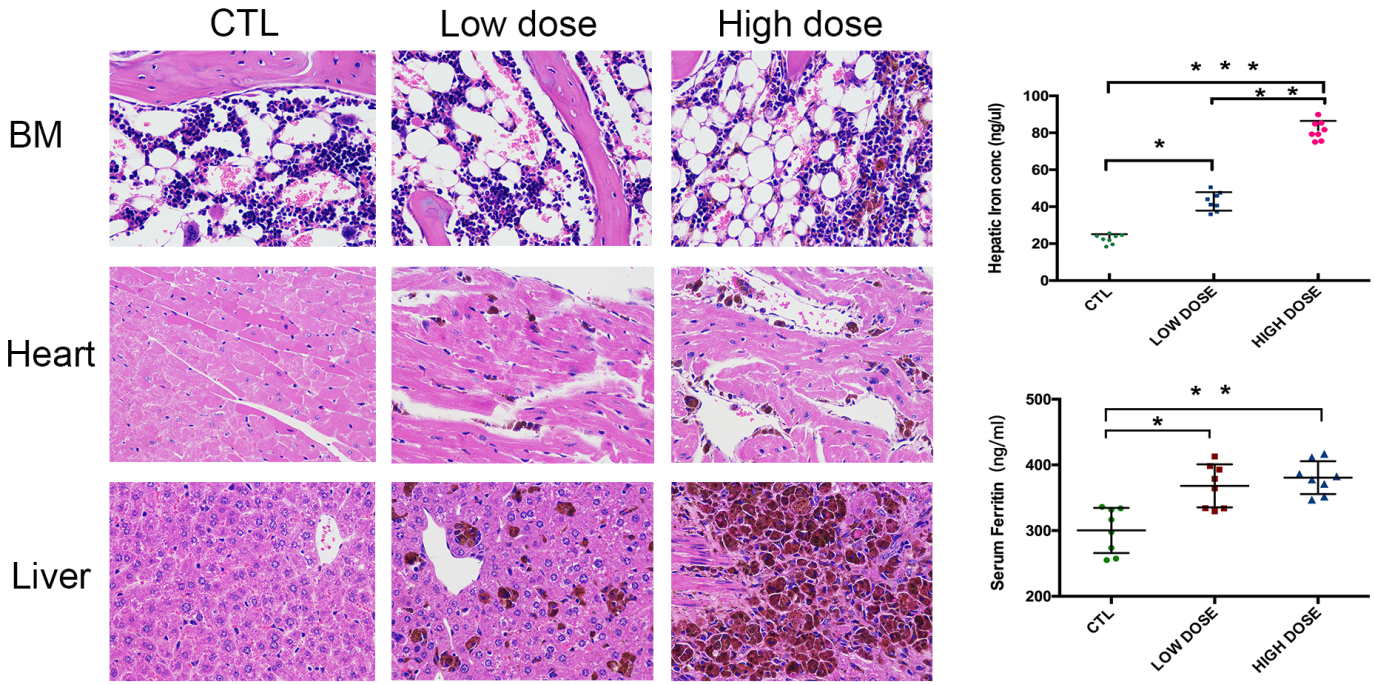

Figure 1

Tissue iron deposition and iron levels in the liver and serum of the iron overload murine model. NOD/SCID mice were injected with escalating doses of iron dextran for 4 weeks. (A) H&E staining was used to examine iron deposition (arrow) in bone marrow, heart, and liver. Iron levels were measured in the liver (B) and serum ferritin (C) using commercially available assay kits. *P<0.05, **P<0.01, ***P<0.001

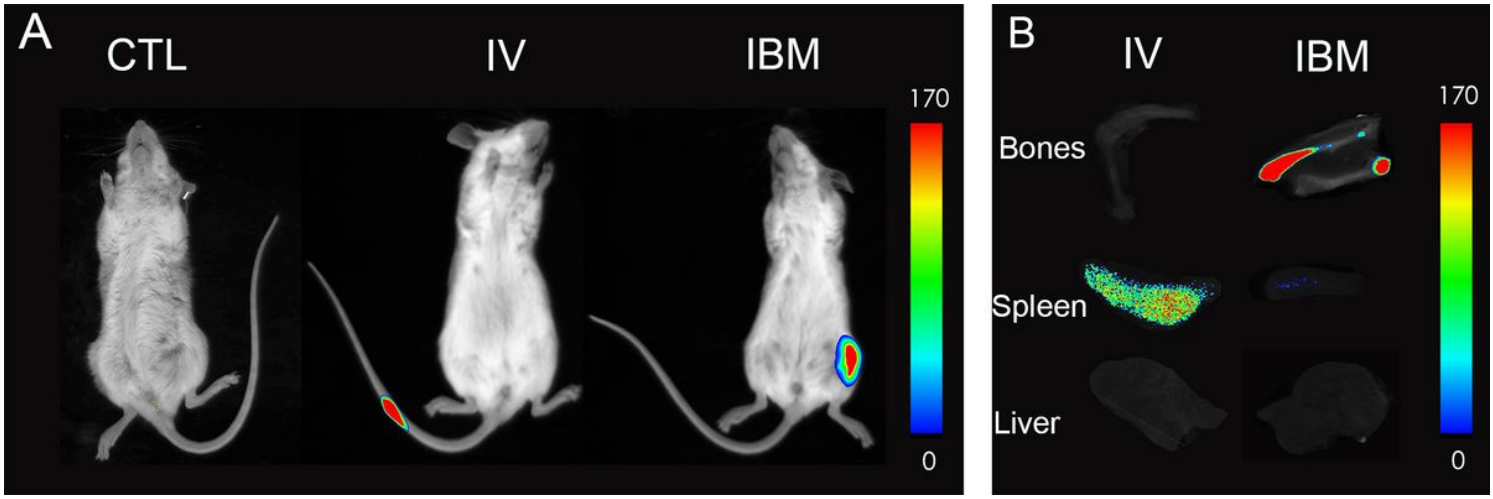

Figure 2

Distribution of UCB-MNC in vivo after transplantation. Intravenous (IV group) or intra-bone marrow (IBM group) injection of DiR-labeled UCB-MNC was via tail vein or tibia, respectively. On the day of transplantation (A) and six weeks after transplantation (B), in vivo fluorescence imaging was performed.

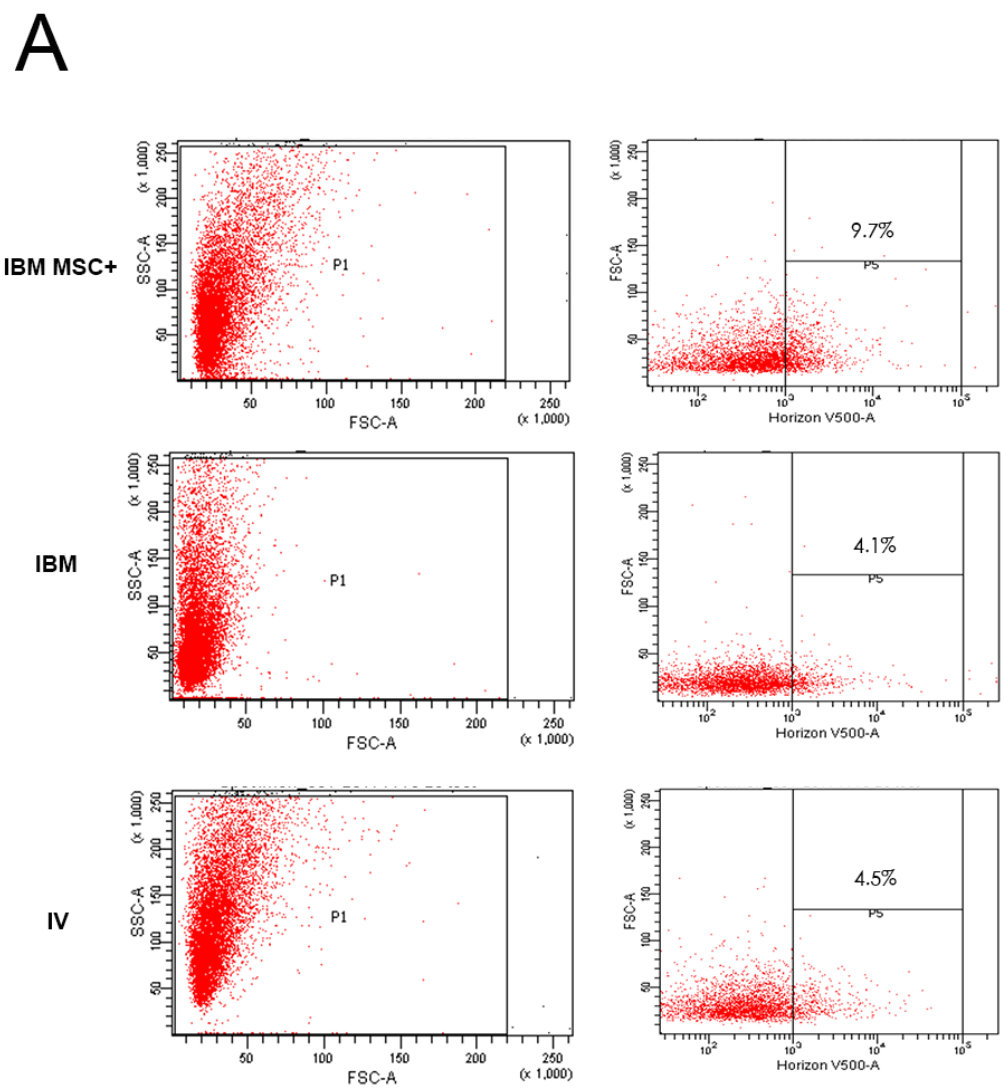

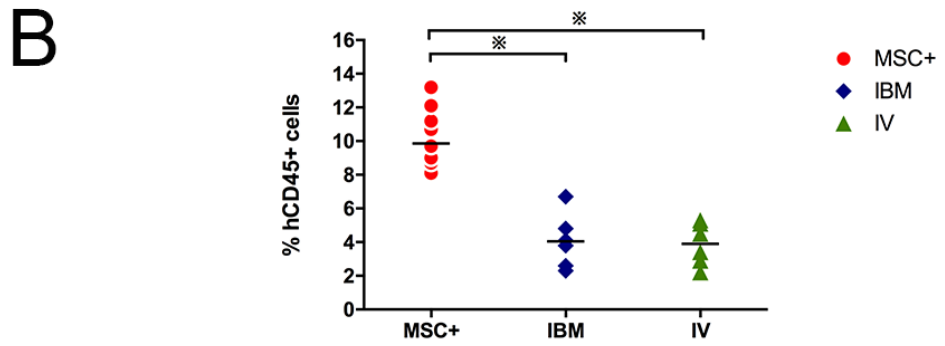

Figure 3

Content of human CD45+ cells in the bone marrow after transplantation. Six weeks after transplantation, the bone marrow of the survived mice in each group was harvested and examined for the content of human CD45+ cells by using flow cytometry. (A) IBM MSC+ group received combined UCB-MNC and UC-MSC via IBM injection, (B) IBM group received only UCB-MNC via IBM injection, and (C) IV group received

only UCB-MNC via intravenous injection. (D) The mean values of the % of CD45+ cells were shown as grouped dot plot. *P<0.05

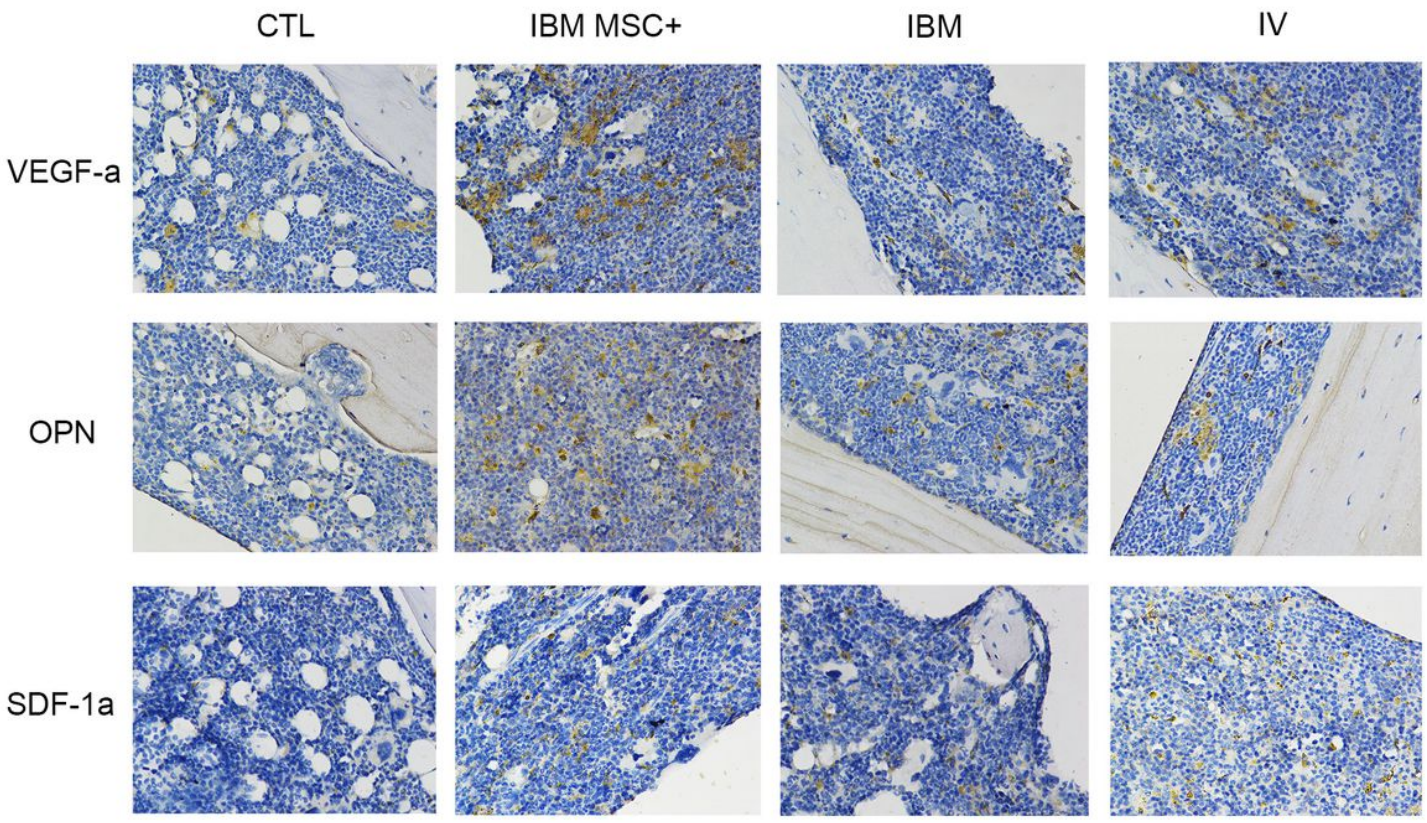

Figure 4

Expression of VEGF-a, OPN, and SDF-1a in the bone marrow after transplantation. Six weeks after transplantation, the bone marrow of the survived mice in each group was harvested and stained for VEGF-a, OPN, SDF-1a expression by using IHC staining. The brown precipitate indicates the presence of positive expression.